Role of the Covalent Glutamic Acid 242−Heme Linkage in the Formation and Reactivity of Redox Intermediates of Human Myeloperoxidase†

Martina Zederbauer,‡ Walter Jantschko,‡ Karin Neugschwandtner,‡ Christa Jakopitsch,‡ Nicole Moguilevsky,§ Christian Obinger,‡ and Paul Georg Furtmüller*,‡

Department of Chemistry, Division of Biochemistry, BOKU−University of Natural Resources and Applied Life Sciences, Muthgasse 18, A-1190 Vienna, Austria, and Head of Technology Transfer Office, University of Namur, 53 Rue de Bruxelles, B-5000 Namur, Belgium

Received January 28, 2005; Revised Manuscript Received March 15, 2005

ABSTRACT: In human myeloperoxidase the heme is covalently attached to the protein via two ester linkages between the carboxyl groups of Glu242 and Asp94 and modified methyl groups on pyrrole rings A and C of the heme as well as a sulfonium ion linkage between the sulfur atom of Met243 and the β-carbon of the vinyl group on pyrrole ring A. In the present study, wild-type recombinant myeloperoxidase (recMPO) and the variant Glu242Gln were produced in Chinese hamster ovary cells and investigated in a comparative sequential-mixing stopped-flow study in order to elucidate the role of the Glu242−heme ester linkage in the individual reaction steps of both the halogenation and peroxidase cycle. Disruption of the ester bond increased heme flexibility, blue shifted the UV−vis spectrum, and, compared with recMPO, decelerated cyanide binding (1.25×10^4 versus 1.6×10^6 M^{-1} s^{-1} at pH 7 and 25 °C) as well as compound **I** formation mediated by either hydrogen peroxide (7.8×10^5 versus 1.9×10^7 M^{-1} s^{-1}) or hypochlorous acid (7.5×10^5 versus 2.3×10^7 M^{-1} s^{-1}). The overall chlorination and bromination activity of Glu242Gln was 2.0% and 24% of recMPO. The apparent bimolecular rate constants of compound **I** reduction by chloride (65 M^{-1} s^{-1}), bromide (5.4×10^4 M^{-1} s^{-1}), iodide (6.4×10^5 M^{-1} s^{-1}), and thiocyanate (2.2×10^5 M^{-1} s^{-1}) were 500, 25, 21, and 63 times decreased compared with recMPO. By contrast, Glu242Gln compound **I** reduction by tyrosine was only 5.4 times decreased, whereas tyrosine-mediated compound **II** reduction was 60 times slower compared with recMPO. The effects of exchange of Glu242 on electron transfer reactions are discussed.

Myeloperoxidase (donor, hydrogen peroxide oxidoreductase, EC 1.11.1.7) (MPO)[1] plays an important role in the unspecific antimicrobial defense system. It is encoded by a single gene on chromosome 17, expressed exclusively during the promyelocytic stage of myeloid differentiation, and stored in the azurophilic granules of mammalian neutrophils (*1*, *2*). It is released during phagocytosis and catalyzes the hydrogen peroxide-mediated oxidation of halide ions and thiocyanate to hypohalous acids and hypothiocyanate (*3*, *4*), which are effective antimicrobial agents. Upon producing these oxidants, MPO has also enormous potential to inflict tissue damage and to induce inflammation (*5*).

Myeloperoxidase belongs to the mammalian peroxidase superfamily including also eosinophil peroxidase (EPO), lactoperoxidase (LPO), and thyroid peroxidase (TPO). MPO is a glycosylated homodimer of 140 kDa [$(\alpha\beta)_2$], each half being composed of 466 amino acids (heavy chain, α) and 108 amino acids (light chain, β) and covalently linked by a disulfide bond with the other identical half (*6*). Each half-molecule contains a covalently bound modified heme. The heme is a derivative of protoporphyrin IX in which the methyl groups on pyrrole rings A and C had been modified to allow formation of ester linkages with Glu242 and Asp94, respectively. A third covalent link was identified as a sulfonium linkage between the sulfur atom of Met243 and the terminal β-carbon of the vinyl group on pyrrole ring A (Figure 1A) (*6*). The presence of the latter has been confirmed by mass spectrometric analysis of the heme released by autolytic cleavage and protease digestion (*7*). In the homologous mammalian peroxidases (EPO, LPO, TPO) there is evidence that the heme is also covalently attached to the protein via two ester linkages and that the cross-linking process is thought to occur autocatalytically, with the 5-hydroxymethyl bond formed before the 1-hydroxymethyl bond (*8*−*11*). These differences in heme linkage within the mammalian peroxidase superfamily are responsible for their distinct optical properties and could be a major factor in the observed differences in substrate specificity (*12*−*14*).

A major breakthrough for the elucidation of structure−function relationships in human peroxidases was the production of a sufficient amount of recombinant MPO (recMPO) in Chinese hamster ovary cell lines (*15*). Secreted recMPO

† This work was supported by the Austrian Science Fund (Project P15660).

* Corresponding author. Telephone: +43-1-36006-6077. Fax: +43-1-36006-6059. E-mail: paul.furtmueller@boku.ac.at.

‡ University of Natural Resources and Applied Life Sciences.

§ University of Namur.

[1] Abbreviations: MPO, mature dimeric myeloperoxidase; recMPO, wild-type recombinant unprocessed monomeric myeloperoxidase; LPO, lactoperoxidase; EPO, eosinophil peroxidase; TPO, thyroid peroxidase; MPO-I, compound **I**; MPO-II, compound **II**; X^-, halide; HOX, hypohalous acid; CHO, Chinese hamster ovary.

10.1021/bi0501737 CCC: $30.25
Published on Web 04/09/2005

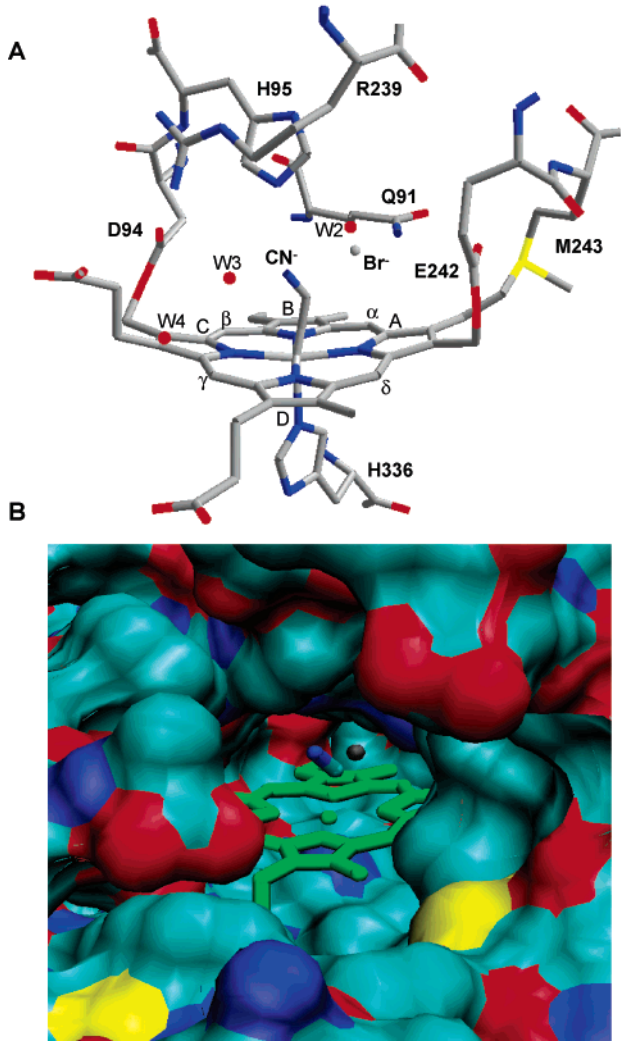

FIGURE 1: (A) Active site structure of human myeloperoxidase complexed with cyanide and with bound bromide. The figure was constructed using the coordinates deposited in the Protein Data Bank (accession code 1D7W). The covalent heme to protein linkages including glutamate 242 are shown. (B) View through the access channel to the active site (complexed with cyanide and with bound bromide) showing exposure of the heme pyrrole ring D. The figure was constructed using VMD (version 1.8.2) (*35*).

is a single-chain precursor of 84 kDa. The protein fails to undergo proteolytic processing into mature subunits and is expressed only in the monomeric form. However, the spectral and kinetic features of monomeric recMPO are identical to those of the homodimeric enzyme purified from the neutrophils (*16*−*18*). Kooter and colleagues investigated the consequences of exchange of Asp94, Glu242, and Met243 on the spectral features and the overall chlorination and peroxidase activity of the corresponding variants (*19*−*21*). Exchange of Met243 by threonine (human EPO), glutamine (bovine LPO), and valine (human TPO) caused a significant or even complete loss of the chlorination activity as well as a blue shift of the Soret band of 14−18 nm, underlining the role of the vinyl sulfonium band in the unusual spectroscopic properties of MPO (*17*). Exchanges of Asp94 resulted in the formation of two distinct species, one with spectral characteristics of wild-type recMPO and one with spectral features similar to the Met243 variants and with chlorination activities of 33% (Asp94Asn) or 2% (Asp94Val) compared to wild-type recMPO (*20*). The loss of the Glu242 ester bond caused a blue shift in the absorption spectrum and loss in the chlorination activity of more than 90% (*20*).

However, a comprehensive examination of the role of these amino acids in MPO catalysis needs the investigation of these mutations on the individual reaction steps of MPO. The simplest reaction is reversible binding of high-spin and low-spin ligands to the ferric enzyme (reaction 1). Upon reaction with hydroperoxides MPO undergoes a two-electron oxidation to form compound **I** in which a porphyrin π-cation radical contains a ferryl(+IV) iron liganded to oxygen (reaction 2) (*22*, *23*). Halides (X^-) reduce compound **I** directly to native MPO by a two-electron process (reaction 3), thereby forming hypohalous acids (HOX) (*12*−*14*).

$$[Fe(III)(Porph)] + X^- \leftrightarrows [Fe(III)(Porph)]X^- \quad (1)$$

$$[Fe(III)(Porph)] + ROOH \leftrightarrows [Fe(IV)=O(Porph)^{\bullet+}] + ROH \quad (2)$$

$$[Fe(IV)=O(Porph)^{\bullet+}] + X^- + H^+ \leftrightarrows [Fe(III)(Porph)] + HOX \quad (3)$$

$$[Fe(IV)=O(Porph)^{\bullet+}] + AH_2 \leftrightarrows [Fe(IV)=O(Porph)] + {}^{\bullet}AH \quad (4)$$

$$[Fe(IV)=O(Porph)] + AH_2 \leftrightarrows [Fe(III)(Porph)] + {}^{\bullet}AH + H_2O \quad (5)$$

$$[Fe(IV)=O(Porph)^{\bullet+}] + H_2O_2 \leftrightarrows [Fe(IV)=O(Porph)] + O_2^{\bullet-} + H^+ \quad (6)$$

$$[Fe(IV)=O(Porph)] + H_2O_2 \leftrightarrows [Fe(III)(O_2^{\bullet-})] + H_2O \quad (7)$$

Alternatively, compound **I** is reduced to the ferric enzyme via compound **II** by two successive one-electron reductions (reactions 4 and 5) releasing free radicals ($^{\bullet}AH$) (*23*). MPO-typical is the oxidaton of H_2O_2 to superoxide (*24*−*26*) (reaction 6), whereas the H_2O_2-mediated conversion of compound **II** to compound **III** (reaction 7) occurs in all heme peroxidases (*23*).

In the present paper we have examined the role of Glu242 in reactions 1−7. By using the multimixing stopped-flow technique the spectral and kinetic features of the ferric protein, compound **I**, compound **II**, and compound **III** of Glu242Gln have been investigated, giving new insights into the structural and functional peculiarities of myeloperoxidase.

EXPERIMENTAL PROCEDURES

Materials. Transfection of recombinant plasmids into Chinese hamster ovary cells, selection and culture procedures for transfected cells, and protein purification protocols were described in detail previously (*15*). The variant Glu242Gln was produced as described by Kooter et al. (*20*) and had a purity index (A_{418}/A_{280}) of about 0.7. The concentration of Glu242Gln was calculated by using the extinction coefficient of 85 mM^{-1} cm^{-1} at 418 nm, which was obtained from the plot of absorbance at 418 mm versus protein concentration obtained by the method of Bradford (*27*). Hydrogen peroxide, obtained as a 30% solution from Sigma Chemical Co., was

diluted and the concentration determined by absorbance measurement at 240 nm where the extinction coefficient is 39.4 M^{-1} cm^{-1} (*28*). Hypochlorous acid was obtained from Fluka. The HOCl stock solutions were prepared in 5 mM NaOH and stored in the dark. The HOCl concentration was determined spectrophotometrically ($\epsilon = 350$ M^{-1} cm^{-1} at 292 nm in 5 mM NaOH) shortly before the experiments (*29*). Peroxide and HOCl stock solutions were prepared freshly half-daily. Cyanide, tyrosine, and ascorbate and all other chemicals were also purchased from Sigma Chemical Co. at the highest grade available.

Circular Dichroism Spectrometry. CD spectra were performed on a Jasco J-600 instrument, equipped with a thermostated cell holder, and data were recorded on-line using a personal computer. Spectra are averages of 12 scans with subtraction of the baseline. The quartz cuvette used had a path length of 2 mm. Samples were measured at 25 °C in 5 mM phosphate buffer, pH 7.0, and with protein concentrations of 2.6 μM.

Steady-State Experiments. Halogenation activity was measured spectrophotometrically (Hitachi U-3000) using the monochlorodimedone (MCD) assay (*30*). MCD (100 μM) was dissolved in 100 mM phosphate buffer, pH 7.0, containing either bromide (100 mM) or chloride (100 mM) and recMPO or Glu242Gln. Upon addition of 100 μM H_2O_2 MCD was converted into dichlorodimedone. Rates of halogenation were determined from the initial linear part of the time traces using an extinction coefficient for MCD at 290 nm of 19.9 mM^{-1} cm^{-1} (*30*).

Various one-electron donors were used to test the effect of exchange of Glu242 on the peroxidase activity (100 mM phosphate buffer, pH 7.0). Ascorbate oxidation (100 μM ascorbate, 100 μM H_2O_2, 100 nM recMPO or Glu242Gln, 25 °C) was followed by a decrease of absorbance at 290 nm using an extinction coefficient for ascorbate of $\epsilon_{290} = 2.8$ mM^{-1} cm^{-1} (*31*). Guaiacol oxidation (100 μM guaiacol, 100 μM H_2O_2, 100 nM recMPO or Glu242Gln, 25 °C) was followed by absorbance increase at 470 nm by using an extinction coefficient of $\epsilon_{470} = 26.6$ mM^{-1} cm^{-1} (*32*). Dityrosine formation from tyrosine (200 μM tyrosine, 100 μM H_2O_2, 50 nM recMPO or Glu242Gln, 25°C) was followed spectrofluorometrically on a Hitachi F-4500 spectrofluorometer using an excitation wavelength of 325 nm and an emission wavelength at 405 nm (*33*).

Equilibrium binding of cyanide to wild-type recMPO or Glu242Gln was performed by spectroscopic titration of 630 nM enzyme in 100 mM phosphate buffer, pH 7.0, with increasing concentrations of cyanide (0.125−314 μM) and plotting the reciprocal of the absorbance difference (peak maximum minus valley) against the ligand/heme ratios.

Transient-State Experiments. The stopped-flow apparatus (model SX-18MV) equipped for both conventional and sequential stopped-flow measurements was from Applied Photophysics. For a total of 100 μL/shot into the optical observation cell with 1 cm light path, the fastest time for mixing two solutions and recording the first data point was of the order of 1.3 ms. All measurements were performed at 25 °C.

Cyanide binding and the reaction of the Glu242Gln mutant with H_2O_2 and HOCl was measured in the conventional stopped-flow mode by following the decrease of absorbance at 430 nm (Soret maximum of ferric recMPO) or 418 nm (Soret maximum of ferric Glu242Gln) or at 456 nm (Soret band of cyanide complex of recMPO) or 442 nm (Soret band of cyanide complex of Glu242Gln). In a typical cyanide binding experiment, one syringe contained 1.3 μM Glu242Gln (100 mM phosphate buffer, pH 7.0), and the second syringe contained at least a 40-fold excess of cyanide (100 mM phosphate buffer, pH 7.0). For monitoring compound **I** formation with H_2O_2 or HOCl at either 430 nm (recMPO) or 418 nm (Glu242Gln), one syringe contained 1.3 μM enzyme in 200 mM phosphate buffer, pH 7.0, and the other syringe various concentrations of either H_2O_2 in 5 mM phosphate buffer, pH 7.0, or hypochlorite in 5 mM NaOH. Three determinations were performed for each ligand or oxidant concentration. The mean of the pseudo-first-order rate constants, k_{obs}, was used in the calculation of the second-order rate constants obtained from the slope of a plot of k_{obs} versus ligand or oxidant concentration.

Because of the inherent instability of recMPO compound **I**, the sequential stopped-flow (multimixing) techniques were used for determination of rates of the reaction of compound **I** with one- and two-electron donors. For wild-type recMPO, the conditions were the same as described for the mature enzyme purified from human blood (*12*). In contrast to wild-type recMPO, the Glu242Gln compound could be formed with slight excess of H_2O_2. Typically Glu242Gln (1.3 μM) was premixed with 2 μM H_2O_2 in the aging loop for 2000 ms (100 mM phosphate buffer, pH 7.0). Finally, compound **I** was allowed to react with varying concentrations of electron donors. Halide oxidation was followed by monitoring the absorbance change at 430 nm (wild-type recMPO) or 418 nm (Glu242Gln). Formation of compound **II** mediated by either ascorbate or tyrosine was followed at 456 nm (wild-type recMPO) or 442 nm (Soret band of compound **II** of Glu242Gln).

Reactivity of compound **II** was investigated either by starting with preformed compound **II** or, alternatively, by following the reaction of compound **I** with ascorbate or tyrosine to compound **II** and back to the ferric enzyme. In the latter case the resulting biphasic curves showed the initial formation of compound **II** and then its subsequent reaction with ascorbic acid, causing an exponential decrease in absorbance. For example, in the first procedure 2 μM Glu242Gln was premixed with an equimolar concentration of hydrogen peroxide and a 20-fold excess of homovanillic acid in 100 mM phosphate buffer, pH 7.0. After a delay time of 5 s, compound **II** was allowed to react with varying concentrations of either ascorbate or tyrosine in the same buffer. Compound **II** reduction was followed at 456 or 430 nm (disappearance of wild-type compound **II** or formation of ferric recMPO) and 442 or 418 nm (disappearance of Glu242Gln compound **II** or formation of ferric Glu242Gln). In the second procedure compound **I** of the Glu242Gln mutant was preformed with equimolar concentrations of hydrogen peroxide, and after a delay time of 2000 ms, it was allowed to react with varying concentrations of tyrosine or ascorbic acid, and absorbance changes were followed at 456 nm (wild-type recMPO) or 442 nm (Glu242Gln).

All reactions were also investigated using the diode array detector (Applied Photophysics PD.1) attached to the stopped-flow machine. Normal data sets were analyzed using the Pro-K simulation program from Applied Photophysics, which allowed the synthesis of artificial sets of time-

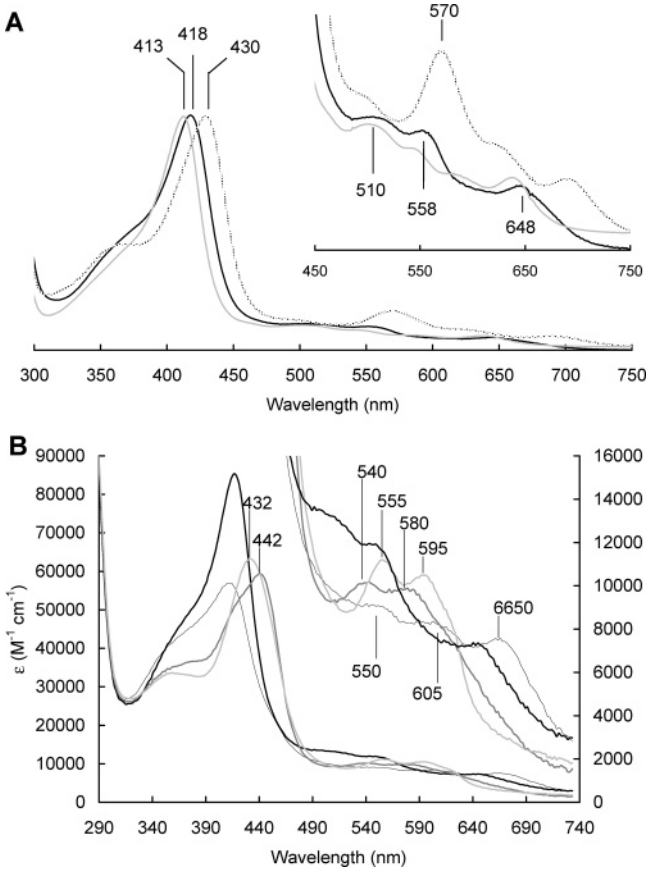

FIGURE 2: (A) Optical absorbance spectra of ferric eosinophil peroxidase (light gray line), recombinant wild-type myeloperoxidase (gray line), and the ferric Glu242Gln mutant (black line) in 5 mM phosphate buffer, pH 7. The RZ values were 1.0 for EPO (A_{413nm}/A_{280nm}), 0.70 for wild-type recMPO (A_{430nm}/A_{280nm}), and 0.70 for Glu242Gln(A_{418nm}/A_{280nm}). (B) Spectra of ferric Glu242Gln (black line), compound **I** (thin line), compound **II** (gray line), and compound **III** (light gray line). For spectral analysis the Pro-K simulation program from Applied Photophysics was used to calculate the Glu242Gln mutant redox intermediates compounds **I** and **II**, using a set of spectral data from a reaction between 2.5 μM Glu242Gln mutant and 250 μM hydrogen peroxide in 100 mM phosphate buffer, pH 7.0 (25 °C). Compound **III** spectra were calculated from a reaction of 2.5 μM Glu242Gln mutant and 5 mM H_2O_2 in 100 mM phosphate buffer, pH 7.0.

dependent spectra as well as spectral analysis of enzyme intermediates.

RESULTS

Electronic Absorption and Circular Dichroism Spectra. The optical absorbance spectra of ferric MPO, Glu242Gln, and EPO are shown in Figure 2A. Wild-type recMPO shows a Soret band at 430 nm and a strong band at 570 nm. By contrast, EPO exhibits a Soret absorbance at 413 nm and weak bands at 500, 550, 560, and 638 nm. As Figure 2A clearly demonstrates, the spectrum of the Glu242Gln is more similar to that of EPO than of MPO. Compared with EPO its Soret band is red shifted to 418 nm, and also the weaker bands in the visible region are red shifted 8−10 nm. The lower purity value of recMPO and Glu242Gln (0.70) compared to the mature homodimeric enzyme (0.88) is caused by an additional polypeptide of 115 residues in unprocessed recMPO.

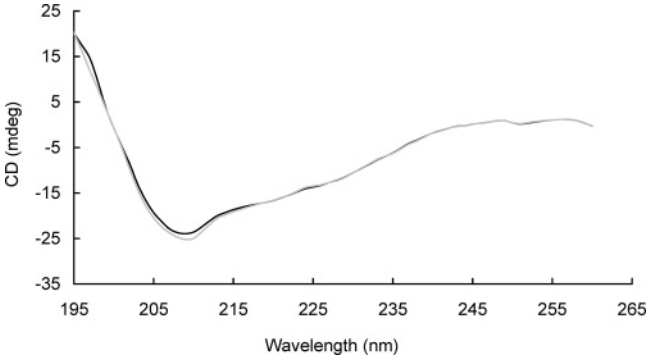

FIGURE 3: Circular dichroism spectra of wild-type recMPO (black line) and Glu242Gln (gray line) measured in 5 mM phosphate buffer, pH 7.0, and 25 °C (protein concentration: 2.6 μM).

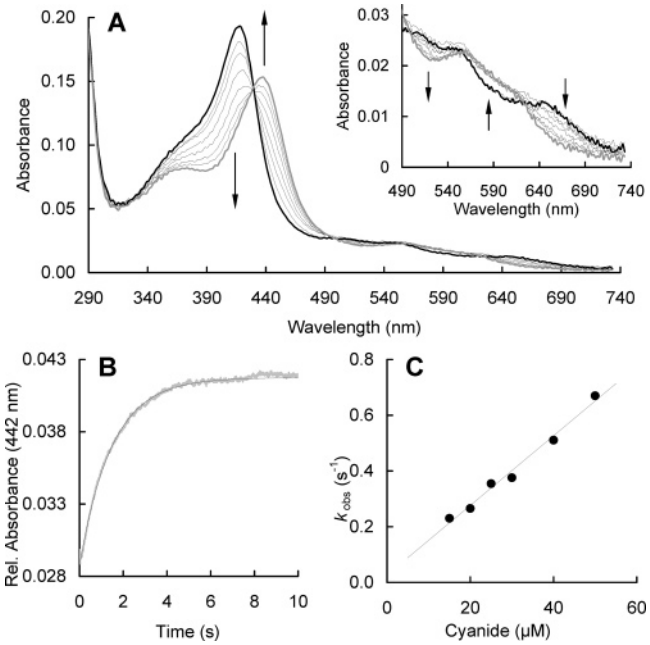

FIGURE 4: Reaction of ferric Glu242Gln with cyanide. (A) Spectral transition of the reaction of 2.5 μM Glu242Gln with 250 μM measured in the conventional stopped-flow mode. The first spectrum shows the ferric mutant in its high-spin state. The second spectrum was recorded 3.8 ms after mixing, with subsequent spectra at 45, 91, 170, 303, 537, and 8690 ms showing the formation of the low-spin cyanide complex. Arrows indicate changes of absorbance with time. Conditions: 100 mM phosphate buffer, pH 7, and 25 °C. (B) Typical time trace at 442 nm and single-exponential fit (1 μM Glu242Gln and 50 μM cyanide). (C) Dependence of k_{obs} values from the cyanide concentration. The association rate constant was calculated from the slope and the dissociation rate constant from the intercept. Final enzyme concentration: 1 μM Glu242Gln in 100 mM phosphate buffer, pH 7.

Figure 3 depicts CD spectra of ferric recMPO and Glu242Gln. The far-UV CD spectra demonstrate that the overall structure is predominantly α-helical and that exchange of glutamate 242 by glutamine did not induce structural changes. If conformational changes did occur, they must have been very localized and minimal and thus went undetected by CD.

Cyanide Binding. Figure 4A shows the spectral changes in Glu242Gln, which occur upon addition of cyanide. Cyanide converts the high-spin ($S = {}^5/_2$) iron state to the low-spin ($S = {}^1/_2$) state, thereby shifting the Soret peak from 418 to 442 nm with a clear isosbestic point at 430 nm. In wild-type recMPO the Soret peak shifted from 430 to 456

Table 1: Overall Chlorination and Bromination Activity of Wild-Type recMPO and Glu242Gln in Comparison with Lactoperoxidase (LPO) in 100 mM Phosphate Buffer, pH 7.0, and 25 °C[a]

	recMPO	Glu242Gln	LPO
chloride (100 mM)			
units/mg	0.893	0.029	0.027
%	100	3.3	3.0
bromide (100 mM)			
units/mg	5.62	2.14	2.84
%	100	38.0	84.5

[a] For details, see Experimental Procedures. One unit is defined as 1 μmol of halide being oxidized per minute.

Table 2: Overall Peroxidase Activity of Wild-Type recMPO and Glu242Gln in Comparison with Lactoperoxidase (LPO) in 100 mM Phosphate Buffer, pH 7.0, and 25 °C[a]

	recMPO	Glu242Gln	LPO
guaiacol			
units/mg	2.05	0.61	6.67
%	100	30	326
ascorbic acid			
units/mg	1.56	2.55	0.91
%	100	163	59
tyrosine			
FU/(min·mg)	6.89×10^5	0.50×10^5	6.64×10^5
%	100	7	96

[a] One unit is defined as 1 μmol of substrate being oxidized per minute. FU = arbitrary fluorescence units obtained from fluorometric monitoring of dityrosine formation.

nm with an isosbestic point at 442 nm (not shown). By using the stopped-flow apparatus, cyanide binding was followed at 442 nm (Glu242Gln) and 456 nm (wild-type recMPO). In both cases cyanide binding was monophasic (Figure 4B). Under conditions of excess of cyanide, pseudo-first-order rate constants, k_{obs}, could be obtained from single-exponential fits. The second-order rate constant (k_{on}) was calculated from the slope of the linear plot of k_{obs} versus cyanide concentration ($k_{obs} = k_{on}[HCN] + k_{off}$; Figure 4C). Cyanide binding to Glu242Gln [$(1.25 \pm 0.07) \times 10^4$ M^{-1} s^{-1} at 25 °C] is about 100 times slower compared to wild-type recMPO [$(1.6 \pm 0.1) \times 10^6$ M^{-1} s^{-1}]. From the intercept of the linear plots (Figure 4C) the dissociation rate constants (k_{off}) were obtained, allowing the calculation of the dissociation constants (K_D) of the cyanide complexes from the k_{off}/k_{on} ratios. Interestingly, the K_D values for wild-type recMPO (1.9 μM) and Glu242Gln (2.4 μM) are similar because the k_{off} values of both proteins differed also by a factor of 100 (3.0 s^{-1} for wild-type recMPO and 0.03 s^{-1} for Glu242Gln).

The K_D for cyanide binding determined by spectroscopic titration was nearly identical with the K_D values obtained from the kinetic experiments. For wild-type recMPO and Glu242Gln K_D values of 1.4 and 3.5 μM were obtained.

Overall Halogenation and Peroxidase Activity. Table 1 summarizes the chlorination and bromination activity of wild-type recMPO, Glu242Gln, and LPO using the MCD assay. Compared with wild-type recMPO (100%), the chlorination activity of both Glu242Gln (3.3%) and LPO (3.0%) was very low, whereas the bromination activity of Glu242Gln was about 38.0% of the wild-type activity.

The effect of exchange of glutamate 242 on the peroxidase activity depended on the nature of the electron donor. Upon using the aromatic substrates guaiacol and tyrosine, the peroxidase activity was diminished by 70% and 93%, respectively, compared to the wild-type enzyme, whereas ascorbate oxidation was even enhanced in Glu242Gln. Table 2 presents these data in comparison with those from LPO measured under identical conditions.

Compound I Formation. Compound **I** of wild-type recMPO is characterized by a 50% decrease of absorbance in the Soret region. At least a 10-fold excess of H_2O_2 is needed to get the full hypochromicity at 430 nm. By contrast, to obtain the full hypochromicity of Glu242Gln, equimolar H_2O_2 is necessary, very similar to both EPO (*13*) and LPO (*14*). Figure 5A shows the formation of Glu242Gln compound **I** which is distinguished from the ferric protein by about 40% hypochromicity and a shift of the Soret band from 418 to 414 nm as well as by absorbance decrease at 510, 558, and 648 nm and the appearance of a new peak at 665 nm (see also Figure 2B). Compound **I** of Glu242Gln is stable for about 2 s and finally decays to an intermediate with spectral features very similar to those of a ferryl-type compound **II** (see inset of Figure 5A) with about 0.8 s^{-1}.

Similar to cyanide binding, the reaction between ferric Glu242Gln and hydrogen peroxide was significantly slower. Under pseudo-first-order conditions the bimolecular rate constant for the compound **I** formation was determined. Figure 5B shows a monophasic exponential time course at 418 nm. In Figure 5C, the k_{obs} values are plotted against hydrogen peroxide concentration. From $k_{obs} = k_{2f}[H_2O_2] + k_{2r}$, the apparent second-order rate constant (k_{2f}) was calculated from the slope of the linear plot [$(7.8 \pm 0.5) \times 10^5$ M^{-1} s^{-1}; intercept $k_{2r} = 0.7$ s^{-1}]. The small intercept suggests that the reverse rate constant, k_{2r}, is negligible. By contrast, the corresponding rates of wild-type recMPO were calculated to be $(1.9 \pm 0.2) \times 10^7$ M^{-1} s^{-1} and 4.4 s^{-1} (Table 3).

Upon using hypochlorous acid to convert ferric recMPO and Glu242Gln, the situation was similar. When HOCl was mixed with the ferric Glu242Gln mutant in the conventional stopped-flow mode, the resulting spectral changes were identical to those obtained with hydrogen peroxide. The monophasic reaction allowed the determination of the bimolecular rate constant to be $(7.5 \pm 0.5) \times 10^5$ M^{-1} s^{-1}, which is also much slower than the corresponding rate of wild-type recMPO: $(2.3 \pm 0.3) \times 10^7$ M^{-1} s^{-1}.

Reactivity of Compound I. The inset in Figure 5A shows the spectral changes of the reaction of ferric Glu242Gln with 250 μM H_2O_2. The rapidly formed compound **I** is transformed to compound **II** with peaks at 442 nm and a twin peak at 540 and 580 nm, which is typical for an oxoferryl (Fe^{IV}=O) species (*23*) (Figure 2B). Isosbestic points between Glu242Gln compound **I** and compound **II** were determined to be at 422, 485, 520, and 610 nm. The maximum absorbance of Glu242Gln compound **II** at 442 nm was about 63% of that of the ferric form at 418 nm, which corresponds to an extinction coefficient ϵ_{442} of 53.6 mM^{-1} cm^{-1}. Isosbestic points in the visible region between compound **II** and ferric Glu242Gln were at 432, 480, 566, and 526 nm.

Compound **II** formation depended strongly on the concentration of H_2O_2. The corresponding time traces displayed a single-exponential character (Figure 5D). From the linear plot of k_{obs} against H_2O_2 concentration (Figure 5E), the apparent second-order rate constant was determined to be $(1.4 \pm 0.1) \times 10^3$ M^{-1} s^{-1} at pH 7.0, which is about 20

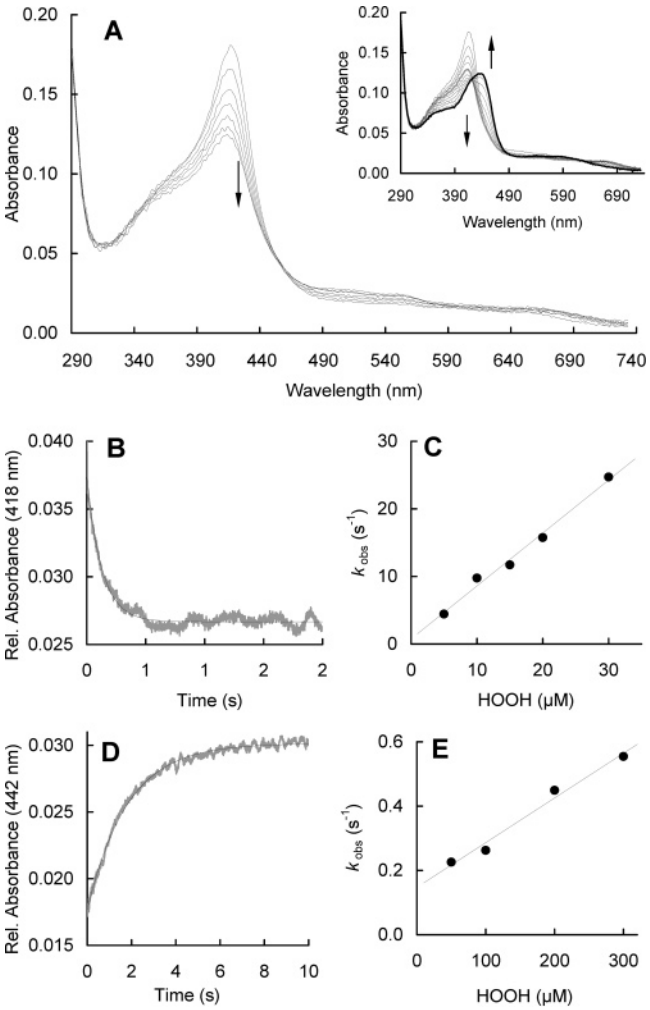

FIGURE 5: Reaction of ferric Glu242Gln with hydrogen peroxide. (A) Spectral transitions upon mixing of 2.5 μM ferric Glu242Gln with 4 μM hydrogen peroxide. The first spectrum was taken 1.3 ms after mixing, with subsequent spectra at 37, 73, 109, 183, 303, and 820 ms. Arrows show the direction of absorbance changes with time. Conditions: 100 mM phosphate buffer, pH 7, and 25 °C. The inset to panel A shows the spectral transition after mixing of 2.5 μM ferric Glu242Gln with 250 μM H_2O_2. The first spectrum was taken 1.3 ms after mixing, with subsequent spectra at 3.8 ms, 6.4 ms, 11.5 ms, 55 ms, 316 ms, 654 ms, 1.33 s, 2.7 s, 5.36 s, and 10.7 s. The spectrum of compound **I** is highlighted in gray and that of compound **II** in black. Arrows indicate absorbance changes with time. (B) Typical time trace and fit of the reaction of ferric Glu242Gln with 20 μM H_2O_2 followed at 418 nm (conditions as in panel A). (C) Pseudo-first-order rate constants for compound **I** formation plotted against hydrogen peroxide concentration. Final enzyme concentration: 0.63 μM in 100 mM phosphate buffer, pH 7, at 25 °C. (D) Typical time trace and fit of the reaction of Glu242Gln compound **I** with 300 μM H_2O_2. The reaction was monitored at 442 nm. (E) Pseudo-first-order rate constants for compound **II** formation plotted against hydrogen peroxide concentration. Conditions as in panel C.

times slower than the reaction of wild-type recMPO compound **I** with H_2O_2. The finite intercept of the plot represents the rate of the spontaneous decay of Glu242Gln compound **I** (0.15 ± 0.03 s^{-1}). Oxidation of H_2O_2 to superoxide by compound **I** is typical for myeloperoxidase (reaction 6) (*26*). Neither EPO (*13*) nor LPO (*14*) can catalyze this reaction. Exchange of Glu242 significantly decreased the rate of H_2O_2 oxidation by compound **I**, but the variant was still able to catalyze the reaction.

Table 3: Apparent Second-Order Rate Constants for Reactions of Wild-Type recMPO and Glu242Gln in Comparison with Eosinophil Peroxidase (EPO) and Lactoperoxidase (LPO)[a]

reaction/substrate	recMPO $\times 10^4$ (M^{-1} s^{-1})	Glu242Gln $\times 10^4$ (M^{-1} s^{-1})	EPO[b] $\times 10^4$ (M^{-1} s^{-1})	LPO[c] $\times 10^4$ (M^{-1} s^{-1})
native enzyme → C-I				
H_2O_2	1900	78	4300	1100
HOCl	2300	75	5600	3200
C-I → native enzyme				
chloride	3.6	0.0065	0.31	NR
bromide	140	5.4	1900	4.1
iodide	1400	64	9300	12000
thiocyanate	1400	22	10000	20000
C-I → C-II				
H_2O_2	3.0	0.14	NR	NR
tyrosine	32	7.4	35	11[d]
ascorbate	23	34	100	
C-II → native enzyme				
tyrosine	1.7	0.028	0.67	1[d]
ascorbate	1.4	2. 1	2.7	
C-II → C-III				
H_2O_2	0.0110	0.0180	0.0211	0.0220

[a] For details, see Experimental Procedures. Abbreviations: C-I, compound **I**; C-II, compound **II**; native enzyme, ferric resting state. NR = no reaction. [b] Reference *13*. [c] Reference *14*. [d] Reference *34*.

Upon adding 5 mM hydrogen peroxide to Glu242Gln compound **I**, compound **II** was formed and, finally, transformed to compound **III** (Figure 2B, light gray line) with a rate of 180 M^{-1} s^{-1} (not shown). Glu242Gln compound **III** is characterized by a Soret peak at 432 nm and a characteristic double peak at 555 and 595 nm in the visible region.

Since Glu242Gln compound **I** was not stable, the sequential-mixing technique had to be used to study its reactivity with halides and thiocyanate as described in Experimental Procedures. Figure 6A shows the bromide-mediated two-electron reduction of Glu242Gln compound **I** to the ferric enzyme. Typical kinetic traces displayed single-exponential character (Figure 6B). In Figure 6C, the dependence of the k_{obs} values from the bromide concentration is shown. Similar plots were also obtained for thiocyanate, iodide, and also chloride (Table 3). Iodide was the best electron donor for Glu242Gln compound **I**, $(6.4 \pm 1.0) \times 10^5$ M^{-1} s^{-1}, followed by thiocyanate, $(2.2 \pm 0.4) \times 10^5$ M^{-1} s^{-1}, and bromide, $(5.4 \pm 0.8) \times 10^4$ M^{-1} s^{-1}, respectively. By contrast, chloride was a very bad electron donor, $(6.5 \pm 0.3) \times 10^1$ M^{-1} s^{-1}, for Glu242Gln compound **I**. The values of the intercepts of the plots of k_{obs} versus halide concentration were very small, ranging from 8 s^{-1} (thiocyanate) to 0.8 s^{-1} (chloride), which is indicative for a clear reaction without side reactions. This is also evident from the full re-increase in absorbance at 418 nm (Figure 6A). In general, exchange of glutamate by glutamine affected the reactivity of compound **I** toward all (pseudo)halides. Compared with wild-type recMPO the rates decreased significantly, ranging from iodide (factor 21) to bromide (factor 25) to thiocyanate (factor 63) to chloride (factor 500).

Upon addition of ascorbic acid or tyrosine to Glu242Gln compound **I** the sequential formation of compound **II** and ferric enzyme was observed. Figure 7A shows the direct spectral transition starting with compound **I** (black line) to compound **II** (gray line) and then the conversion back to ferric Glu242Gln. The transition of compound **I** to compound **II** showed defined isosbestic points at 410 and 632 nm

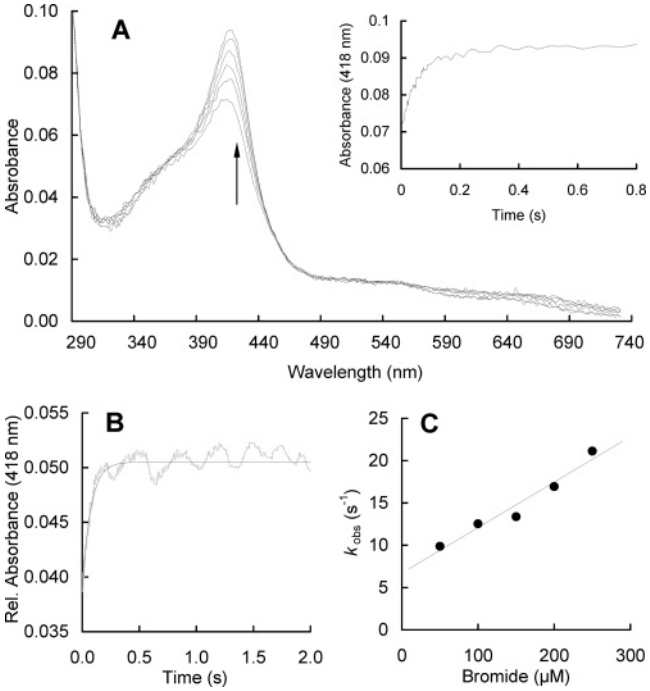

FIGURE 6: Reaction of Glu242Gln compound **I** with bromide. (A) Spectral transitions upon addition of 250 μM bromide to Glu242Gln compound **I** (1.3 μM) in the sequential mixing mode. Compound **I** was preformed with a slight excess of H_2O_2 as described in Experimental Procedures. The first spectrum was recorded 1.3 ms after mixing, with subsequent spectra at 19, 37, 73, 183, and 821 ms. The reaction was carried out in 100 mM phosphate buffer, pH 7.0, and 25 °C. (B) Typical time trace and fit of the reaction of Glu242Gln compound **I** with 150 μM bromide followed at 418 nm. Final conditions were 0.63 μM Glu242Gln mutant and 1 μM H_2O_2, 100 mM phosphate buffer, pH 7.0, and 25 °C. (C) Pseudo-first-order rate constants plotted against bromide concentration.

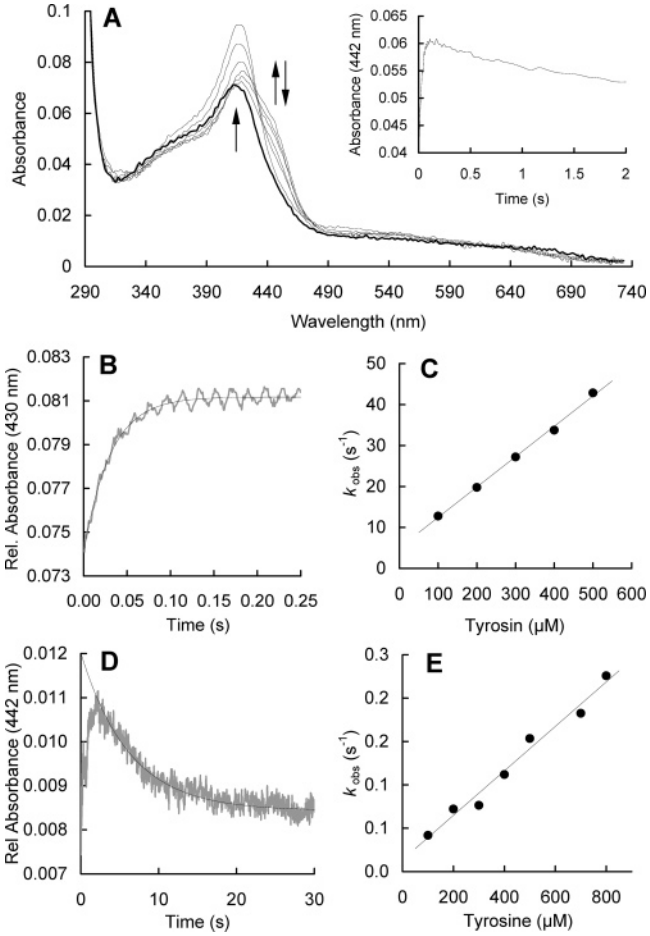

FIGURE 7: Reduction of Glu242Gln compound **I** and compound **II** by tyrosine. (A) Spectral changes upon addition of 500 μM tyrosine to 2.5 μM compound **I** in the sequential-mixing stopped-flow mode. Compound **I** was formed by mixing 5 μM ferric Glu242Gln mutant with 8 μM H_2O_2 and waiting for 2000 ms. The first spectrum was recorded at 1.3 ms, with subsequent spectra at 24 ms, 47 ms, 227 ms, 1.54 s, 5.36 s, and 10 s. The inset shows the biphasic time trace at 442 nm, the absorbance maximum of Glu242Gln compound **II**. Reaction conditions: 100 mM phosphate buffer, pH 7.0, and 25 °C. (B) Typical monophasic time trace with a single-exponential fit showing the reaction of Glu242Gln compound **I** with 400 μM tyrosine followed at 430 nm, the isosbestic point between compound **II** and the ferric protein. (C) Pseudo-first-order rate constants for Glu242Gln compound **I** reduction by tyrosine plotted against tyrosine concentration. (D) Single-exponential fit of the second slower phase of the biphasic time trace at 442 nm obtained from the reaction of Glu242Gln compound **I** with tyrosine. (E) Dependence of k_{obs} values of tyrosine-mediated compound **II** reduction from the tyrosine concentration.

whereas the transition of compound **II** to ferric Glu242Gln exhibits isosbestic points at 430 and 632 nm. The inset to Figure 7A and as well as Figure 7D shows the typical biphasic time trace observed at 442 nm, which was obtained when Glu242Gln compound **I** was mixed with either ascorbate or tyrosine. After initial formation of compound **II** (Soret maximum at 442 nm) the reaction continues and ferric Glu242Gln was formed (decrease at 442 nm), indicating that both redox intermediates react with these one-electron donors. The conversion of compound **I** to compound **II** was followed at 430 nm because there is no contribution from the consecutive reaction. The resulting time traces displayed single-exponential character (Figure 7B), and the apparent second-order rate constants were determined from the corresponding linear plots (Figure 7C) to be $(3.4 \pm 0.3) \times 10^5$ M^{-1} s^{-1} (ascorbate) and $(7.4 \pm 0.2) \times 10^4$ M^{-1} s^{-1} (tyrosine). Compared to wild-type recMPO compound **I**, the reactivity of Glu242Gln compound **I** toward tyrosine was decreased by a factor of 5, but interestingly, the reactivity toward ascorbate was increased (Table 3).

Compound **II** reduction was followed at 442 nm. Figure 7D shows a typical time trace of the reaction of Glu242Gln compound **I** with tyrosine, showing formation and reduction of compound **II**. From single-exponential curve fits, pseudo-first-order rate constants, k_{obs}, were obtained from the latter part of the curve. The corresponding linear plot (Figure 7E) yielded a second-order rate constant of $(2.8 \pm 0.2) \times 10^2$ M^{-1} s^{-1} for tyrosine and $(2.1 \pm 0.2) \times 10^4$ M^{-1} s^{-1} for ascorbic acid. The intercepts were close to zero within experimental error. Similarly to compound **I** reduction, compound **II** reduction by ascorbate was increased with Glu242Gln compared to wild-type recMPO, whereas the reactivity toward tyrosine was significantly decreased.

Very similar rates for compound **II** reduction were obtained when preformed compound **II** was mixed with either ascorbate or tyrosine. A good preparation of Glu242Gln compound **II** was achieved with an equimolar concentration of hydrogen peroxide and at least a 20-fold excess of homovanillic acid (HVA). Addition of HVA was necessary, because in the absence of an electron donor compound **I** was slowly transformed to a compound **II**-like species, which

could differ from the pure ferryl-type compound **II** by being still two oxidizing equivalents above the resting state of the enzyme. HVA is a good electron donor for Glu242Gln mutant compound **I** with a bimolecular rate constant of (7.5 ± 0.5) × 10^4 M^{-1} s^{-1} but did not react with compound **II**.

DISCUSSION

One of the most interesting features of mammalian peroxidases is the extraordinary nature of their prosthetic group. The covalent links are responsible for the low symmetry and bowed distortion from the planar conformation of the heme group (Figure 1A) and the spectroscopic and kinetic peculiarities of these peroxidases (*1*). Since the consequences of each single link on the reactivity of the individual redox intermediates have not been investigated so far, we perfomed this study to elucidate the influence of the loss of the Glu242 ester bond on the reactivity of the individual redox intermediates.

Loss of the Glu242 ester bond resulted in a blue shift of the Soret band due to a rearrangement of the bowed heme structure (*6*), resulting in a more flexible heme of higher symmetry. The red-shifted position of the Soret band of Glu242Gln compared to LPO or EPO is the result of the electron-withdrawing effect of the sulfonium ion linkage, which is still present in this variant as shown by the fact that it is still sensitive to autocleavage of the Met243−Pro244 band (*19*), which is typical for wild-type MPO but not for LPO or EPO. The presence of the sulfonium linkage as well as the higher heme flexibility in Glu242Gln was also indicated by EPR and resonance Raman spectroscopic studies (*20*).

The cyanide complex of a heme peroxidase is a useful analogue of the unstable redox intermediate compound **I**. It has been shown by Lee et al. (*36*) that, at low pH, the low-spin EPR spectrum of the cyanide complex of MPO is altered by halide binding and that the effects of chloride differ substantially from those of bromide and iodide, suggesting halide binding at the distal heme cavity. As shown by the crystal structure of the low-spin cyanide−MPO complex (*37*), cyanide binding causes displacement of the water molecule W1, which is positioned approximately midway between N_ϵ of His95 and the heme iron in ferric MPO. The heme iron to cyanide carbon distance of 2.06 Å and its nitrogen atom form three hydrogen bonds with the distal histidine as well as with the two water molecules W2 and W3. The present stopped-flow study showed that cyanide binding to Glu242Gln exhibits both a significantly lowered association, k_{on}, and dissociation rate constant, k_{off}, compared to the recombinant wild-type MPO; however, K_D remained unchanged. Unchanged K_D values were confirmed by conventional ligand binding titration studies. In other words, the loss of the Glu242 link had a dramatic influence in reaching the equilibrium. By contrast, exchange of Met243 resulted in a dramatic decrease of K_D for the corresponding cyanide complex (*21*), which also supports the presence of the sulfonium ion linkage in Glu242Gln. The drastically reduced k_{off} value of the Glu242Gln cyanide complex indicates strong binding of cyanide to the heme iron and suggests disruption of the three hydrogen bonds observed in the wild-type MPO cyanide complex.

The hydrogen peroxide or hypochlorous acid mediated formation of Glu242Gln compound **I** was decreased to the same extent as cyanide binding. Cyanide binding resembles that of hydrogen peroxide or hypochlorous acid. In both cases the reaction is initiated by deprotonation of either HCN, H_2O_2, or HOCl by the distal histidine followed by binding of the anions (CN^- or ^-OOH or ^-OCl) to the heme iron. In case of compound **I** formation by hydrogen peroxide a transient Fe^{III}−OOH intermediate is formed, followed by fast heterolytic cleavage of the O−O bond, leading to formation of compound **I** and expulsion of a water molecule. Similar to the rate of cyanide binding, the apparent second-order rate constants of compound **I** formation mediated by H_2O_2 and HOCl were about 20−30-fold lower than that of recombinant wild-type MPO, LPO, and EPO (Table 3). These findings suggest that the loss of the Glu242−heme ester bond changes the heme iron to His95 distance at the distal heme cavity, complicating efficient deprotonation and decreasing complex stabilization. Most interestingly, upon addition of 1 equiv of hydrogen peroxide to the ferric Glu242Gln mutant, compound **I** was completely formed, similar to EPO (*13*) and LPO (*14*) but in contrast to wild-type MPO where an excess of H_2O_2 is needed to obtain the full hypochromicity at the Soret absorbance. It was postulated that in wild-type MPO formation of compound **I** is reversible (*25*), as indicated by a relatively high intercept in the plot of k_{obs} versus H_2O_2 concentration (*12*, *25*). In the corresponding plot of Glu242Gln the value of this intercept was within experimental error, which means that the reaction is irreversible. This suggests that loss of heme asymmetry could correlate with a lower standard reduction potential of the compound **I**/ferric MPO couple of Glu242 (since water to hydrogen peroxide oxidation needs a strong oxidant), which is also obvious from the significant loss of the chlorination activity (see below).

Nevertheless, the overall electronic features of Glu242Gln compound **I** as deduced from the UV−vis spectra remained typical for an oxoferryl-type compound **I** in combination with a porphyrinyl radical (*23*). The Glu242Gln variant retained also the MPO-typical feature to catalyze the hydrogen peroxide-dependent transition of compound **I** to compound **II** (i.e., one-electron oxidation of H_2O_2 to superoxide), though exchange of Glu242 by Gln significantly decreased also the rate of this reaction. EPO (*13*) and LPO (*14*) have been shown to be unable to catalyze this reaction. Similar to wild-type MPO, an excess of hydrogen peroxide mediated the transition of Glu242Gln compound **II** to compound **III** in a concentration-dependent manner. The calculated rate (180 M^{-1} s^{-1}) was very similar to that reported for both wild-type MPO (*38*) and LPO (*39*).

Disruption of the ester bond between Glu242 and the heme had also a strong impact on the oxidation of halides. The variant Glu242Gln was still able to oxidize chloride, but both the overall rate (Table 1) and the bimolecular rate constant of the reaction between compound **I** and chloride (Table 3) were significantly decreased. The calculated rate for the chloride oxidation is 550-fold slower compared to wild-type MPO and 48-fold slower compared to EPO. Two explanations are possible: (i) the more flexible heme in Glu242Gln exhibits a lower standard reduction potential of the redox couple compound **I**/ferric peroxidase compared to wild-type MPO, where it has been shown to be 1.16 V at pH 7.0 and 25 °C (*40*) compared to 1.1 V of EPO (*41*). The LPO- and EPO-like stoichiometry of compound **I** formation of Glu242Gln by H_2O_2 supports this hypothesis. On the other

hand, upon loss of the ester bond also the bimolecular rate constants of the reaction of compound **I** with all other (pseudo)halides were decreased (ranging from 22-fold for bromide to 63-fold for thiocyanate compared with wild-type MPO) though oxidation of these two-electron donors is thermodynamically less demanding than chloride oxidation. The overall rate of bromide oxidation is in the same range as for LPO but is 350-fold slower than with EPO. These findings suggest that also (ii) the binding affinity of these (pseudo)halides was affected by disruption of the Glu242 ester bond. Halide binding was shown to occur inside the distal heme cavity in close proximity to the distal histidine (His95) replacing a water molecule (W2) which is hydrogen bonded to the side chain of Gln91, a highly conserved residue in human peroxidases (*6*). It has been shown by Fiedler et al. (*6*) that superposition of the refined MPO−bromide and native model indicates small shifts of the side chains of His95 and the heme ester linked Glu242, which is only 3.5 Å away from W2 in the native enzyme. Possible electrostatic interactions of the bound bromide occur between water molecules W1 and W5, N_ϵ of His95, and the amide nitrogen of Gln91. The closest heme atom to the bromide is the methylene bridge carbon δ (3.8 Å) between pyrrole rings A and D (see also Figure 1). Some differences were observed in the structure of bromide bound to the cyanide complex of MPO, which is a useful model for compound **I**. Bromide bound to the MPO−cyanide complex does not appear to make any significant electrostatic interactions with the protein, the heme, or the bound cyanide (*37*). The closest protein atoms in the crystal structure were shown to be the C_γ atom of Glu242 (3.8 Å) and the C_γ of Arg239 (3.8 Å), and the nearest neighboring heme atom is the pyrrole ring D methyl carbon (4.55 Å) (*37*) (see Figure 1). In addition, there is a marked change in the orientation of the cyanide ion (which is more tilted in the bromide complex). The kinetic findings of the present investigation strongly suggest modifications in these interactions upon disruption of the ester bond to pyrrole ring A. The Glu242 link, together with the Met243 link, seems to optimize the halide positioning for halide oxidation in MPO by putting the halide and/or the heme group in a solid fixed conformation that allows direct electron transfer to the δ-meso carbon of the porphyrin π-cation radical of compound **I**, followed by incorporation of the oxyferryl oxygen into the hypohalous acid product. This mechanism is plausible not only because of the exposure of the δ-meso carbon at the entrance to the distal heme cavity but also from the fact the δ-methine bridge carbon may be particularly electron deficient in compound **I** since it is located adjacent to the positively charged sulfonium ion linkage to the vinyl group attached to pyrrole ring A.

Not only two-electron but also single-electron transfer reactions have been postulated to occur near this δ-methine bridge carbon. This is underlined not only by a decrease in the overall rate of guaiacol and tyrosine oxidation by Glu242Gln (Table 2) but also by a decrease in the individual bimolecular rate constants of compound **I** and compound **II** reduction by tyrosine (Table 3). Single-electron transfer to the heme periphery has been documented in horseradish peroxidase (*42*) but has been also deduced from the X-ray crystal structure of the bisubstrate analogue inhibitor salicylhydroxamic acid (SHA) bound to MPO (*43*). In the MPO−SHA crystal structure, the aromatic ring bound to a hydrophobic region at the entrance to the distal cavity is almost centered above the pyrrole ring D 8-methyl group (*43*). Similar to halide binding, the ester linkage of Glu242 with the heme seems to be important in optimum positioning of the methylene bridge carbon δ for electron transfer from aromatic donors. Interestingly, oxidation of the hydrophilic donor ascorbate by compound **I** and compound **II** was even enhanced in Glu242Gln compared to wild-type MPO (Tables 2 and 3), suggesting a different binding site.

In summary, the Glu242−heme ester linkage is important in maintaining the catalytic activities of human myeloperoxidase. Together with Asp94 and Met243 it is responsible for the asymmetric bow-shaped structure of the heme. Disruption of the Glu242−heme ester linkage increases the flexibility of the prosthetic group, thereby decreasing the rate of reaction of H_2O_2 and cyanide with ferric MPO as well as oxidation reactions of both (pseudo)halides and aromatic electron donors. The kinetic findings suggest an altered heme iron to distal histidine distance as well as an unfavorable change in the position of the heme methylene bridge carbon between pyrrole rings A and D, thereby rendering both heme oxidation and electron transfer to the heme more difficult.

REFERENCES

1. Schultz, J., and Kaminker, K. (1962) Myeloperoxidase of the leucocyte of normal human blood. I. Content and localization, *Arch. Biochem. Biophys. 96*, 465−467.
2. Nauseef, W. M., McCormick, S., and Goedken, M. (2000) Impact of missense mutations on biosynthesis of myeloperoxidase, *Redox Rep. 5*, 197−206.
3. Klebanoff, S. J. (1970) Myeloperoxidase: contribution to the microbicidal activity of intact leukocytes, *Science 169*, 1095−1097.
4. Harrison, J. E., and Schultz, J. (1976) Studies on the chlorinating activity of myeloperoxidase, *J. Biol. Chem. 251*, 1371−1374.
5. Weiss, S. J. (1989) Tissue destruction by neutrophils, *N. Engl. J. Med. 320*, 365−376.
6. Fiedler, T. J., Davey, C. A., and Fenna, R. E. (2000) X-ray crystal structure and characterization of halide-binding sites of human myeloperoxidase at 1.8 Å resolution, *J. Biol. Chem. 275*, 11964−11971.
7. Taylor, K. L., Strobel, F., Yue, K. T., Ram, P., Pohl, J., Woods, A. S., and Kinkade, J. M. (1995) Isolation and identification of a protoheme IX derivative released during autolytic cleavage of human myeloperoxidase, *Arch. Biochem. Biophys. 316*, 635−642.
8. Suriano, G., Watanabe, S., Ghibaudi, E. M., Bollen, A., Ferrari, R. P., and Moguilevsky, N. (2001) Glu375Gln and Asp225Val mutants: about the nature of the covalent linkages between heme group and apo-protein in bovine lactoperoxidase, *Bioorg. Med. Chem. Lett. 11*, 2827−2831.
9. Colas, C., Kuo, J. M., and Ortiz de Montellano, P. R. (2002) Asp-225 and Glu-375 in autocatalytic attachment of the prosthetic heme group of lactoperoxidase, *J. Biol. Chem. 277*, 7191−7200.
10. Oxvig, C., Thomsen, A. R., Overgaard, M. T., Sorensen, E. S., Hojrup, P., Bjerrum, M. J., Gleigh, G. J., and Sottrup-Jensen, L. (1999) Biochemical evidence for heme linkage through esters with Asp-93 and Glu-241 in human eosinophil peroxidase. The ester with Asp-93 is only partially formed in vivo, *J. Biol. Chem. 274*, 16953−16958.
11. Fayadat, L., Niccoli-Sire, P., Lanet, J., and Franc, J.-L. (1999) Role of heme in intracellular trafficking of thyroperoxidase and involvement of H_2O_2 generated at the apical surface of thyroid cells in autocatalytic covalent heme binding, *J. Biol. Chem. 274*, 10533−10538.
12. Furtmüller, P. G., Burner, U., and Obinger C. (1998) Reaction of myeloperoxidase compound I with chloride, bromide, iodide, and thiocyanate, *Biochemistry 37*, 17923−17930.
13. Furtmüller, P. G., Burner, U., Regelsberger, G., and Obinger, C. (2000) Spectral and kinetic studies on the formation of eosinophil peroxidase compound I and its reaction with halides and thiocyanate, *Biochemistry 39*, 15578−15584.

14. Furtmüller, P. G., Jantschko, W., Regelsberger, G., Jakopitsch, C., Arnhold, J. and Obinger, C. (2002) Reaction of lactoperoxidase compound I with halides and thiocyanate, *Biochemistry 41*, 11895−11900.
15. Moguilevsky, N., Garcia-Quintana, L., Jacquet, A., Tournay, C., Fabry, L., Pierard, L., and Bollen, A. (1991) Structural and biological properties of human recombinant myeloperoxidase produced by Chinese hamster ovary cell lines, *Eur. J. Biochem. 197*, 605−614.
16. Jacquet, A., Deby, C., Mathy, M., Moguilevsky, N., Deby-Dupont, G., Thirion, A., Goormaghtigh, E., Garcia-Quintana, L., Mollen, A., and Pincemail, J. (1991) Spectral and enzymatic properties of human recombinant myeloperoxidase: comparison with the mature enzyme, *Arch. Biochem. Biophys. 291*, 132−138.
17. Kooter, I. M., Pierik, A., Merkx, M., Averill, B. A., Moguilevsky, N., Bollen, A., and Wever, R. (1997) Difference Fourier transform infrared evidence for ester bonds linking the heme group in myeloperoxidase, lactoperoxidase, and eosinophil peroxidase, *J. Am. Chem. Soc. 119*, 11542−11543.
18. Furtmüller, P. G., Jantschko, W., Regelsberger, G., Jakopitsch, C., Moguilevsky, N., and Obinger, C. (2001) A transient kinetic study on the reactivity of recombinant unprocessed monomeric myeloperoxidase, *FEBS Lett. 503*, 147−150.
19. Kooter, I. M., Moguilevsky, N., Bollen, A., Sijtsema, N. M., Otto, C., and Wever, R. (1997) Site-directed mutagenesis of Met243, a residue of myeloperoxidase involved in binding of the prosthetic group, *J. Biol. Inorg. Chem. 2*, 191−197.
20. Kooter, I. M., Moguilevsky, N., Bollen, A., Sijtsema, N. M., Otto, C., Dekker, H. L. and Wever, R. (1999) Characterization of the Asp94 and Glu242 mutants in myeloperoxidase, the residues linking the heme group via ester bonds, *Eur. J. Biochem. 264*, 211−217.
21. Kooter, I. M., Moguilevsky, N., Bollen, A., van der Veen, L. A., Otto, C., Dekker, H. L., and Wever, R. (1999) The sulfonium ion linkage in myeloperoxidase. Direct spectroscopic detection by isotopic labeling and effect of mutation, *J. Biol. Chem. 274*, 26794−26802.
22. Dolphin, D., Forman, A., Borg, D. C., Fajer, J., and Felton, R. (1971) Compounds I of catalase and horseradish peroxidase: pication radicals, *Proc. Natl. Acad. Sci. U.S.A. 68*, 614−618.
23. Dunford, H. B. (1999) *Heme Peroxidases*, Wiley-VCH, New York.
24. Hoogland, H., Dekker, H. L., van Riel, C., Kuilenburg, A., Muijsers, A. O., and Wever, R. (1988) A steady-state study on the formation of compounds II and III of myeloperoxidase, *Biochim. Biophys. Acta 955*, 337−345.
25. Marquez, L. A., Huang, J. T., and Dunford, H. B. (1994) Spectral and kinetic studies on the formation of myeloperoxidase compounds I and II: roles of hydrogen peroxide and superoxide, *Biochemistry 33*, 1447−1454.
26. Furtmüller, P. G., Burner, U., Jantschko, W., Regelsberger, G., and Obinger, C. (2000) Two-electron reduction and one-electron oxidation of organic hydroperoxides by human myeloperoxidase, *FEBS Lett. 484*, 139−143.
27. Bradford, M. (1976) A rapid and sensitive method for the quantization of micro quantities of protein utilizing the principle of protein-dye binding, *Anal. Biochem. 72*, 248−254.
28. Nelson, D. P., and Kiesow, L. A. (1972) Enthalpy of decomposition of hydrogen peroxide by catalase at 25 degrees C (with molar extinction coefficients of H_2O_2 solutions in the UV), *Anal. Biochem. 49*, 474−478.
29. Morris, C. (1966) The acid ionization constant of HOCl from 5 to 35°, *J. Phys. Chem. 70*, 3798−3805.
30. Kettle, A. J., and Winterbourn, C. C. (1988) The mechanism of myeloperoxidase-dependent chlorination of monochlorodimedon, *Biochim. Biophys. Acta 957*, 185−191.
31. Nakano, Y., and Asada, K. (1981) Hydrogen peroxide is scavenged by ascorbat-specific peroxidase in spinach chloroplasts, *Plant Cell Physiol. 22*, 867−880.
32. Chance, B., and Maehly, A. C. (1964) Assay of catalases and peroxidases, *Methods Enzymol. 2*, 764−775.
33. Marquez, L. A., and Dunford, H. B. (1995) Kinetics of oxidation of tyrosine and dityrosine by myeloperoxidase compounds I and II. Implications for lipoprotein peroxidation studies, *J. Biol. Chem. 270*, 30434−30440.
34. Jantschko, W., Furtmüller, P. G., Allegra, M., Livrea, M. A., Jakopitsch, C., Regelsberger, G., and Obinger, C. (2002) Redox intermediates of plant and mammalian peroxidases: a comparative transient-kinetic study of their reactivity toward indole derivatives, *Arch. Biochem. Biophys. 396*, 12−22.
35. Humphrey, W., Dalke, A., and Schulten, K. (1996) VMD−Visual Molecular Dynamics, *J. Mol. Graphics 14*, 33−38.
36. Lee, H. C., Booth, K. S., Caughey, W. S., and Ikeda-Saito, M. (1991) Interaction of halides with the cyanide complex of myeloperoxidase: a model for substrate binding to compound I, *Biochim. Biophys. Acta 1076*, 317−320.
37. Blair-Johnson, M., Fiedler, T., and Fenna, R. (2001) Human myeloperoxidase: structure of a cyanide complex and its interaction with bromide and thiocyanate substrates at 1.9 Å resolution, *Biochemistry 20*, 13990−13997.
38. Jantschko, W., Furtmüller, P. G., Zederbauer, M., Lanz, M., Jakopitsch, C., and Obinger, C. (2003) Direct conversion of ferrous myeloperoxidase to compound II by hydrogen peroxide: an anaerobic stopped-flow study, *Biochem. Biophys. Res. Commun. 312*, 292−298.
39. Jantschko, W., Furtmüller, P. G., Zederbauer, M., Neugschwandtner, K., Jakopitsch, C., and Obinger, C. (2005) Reaction of ferrous lactoperoxidase with hydrogen peroxide and dioxygen: an anaerobic stopped-flow study, *Arch. Biochem. Biophys. 434*, 51−59.
40. Arnhold, J., Furtmüller, P. G., Regelsberger, G., and Obinger, C. (2001) Redox properties of the couple compound I/native enzyme of myeloperoxidase and eosinophil peroxidase, *Eur. J. Biochm. 268*, 5142−5148.
41. Furtmüller, P. G., Arnhold, J., Jantschko, W., Pichler, H., and Obinger, C. (2003) Redox properties of the couples compound I/compound II and compound II/native enzyme of human myeloperoxidase, *Biochem. Biophys. Res. Commun. 301*, 551−557.
42. Ator, M. A., and Ortiz de Montellano, P. R. (1987) Protein control of prosthetic heme reactivity. Reaction of substrates with the heme edge of horseradish peroxidase, *J. Biol. Chem. 262*, 1542−1551.
43. Davey, C. A., and Fenna, R. E. (1996) 2.3 Å resolution X-ray crystal structure of the bisubstrate analogue inhibitor salicylhydroxamic acid bound to human myeloperoxidase: a model for a prereaction complex with hydrogen peroxide, *Biochemistry 35*, 10967−10973.

BI0501737